Available online at www.sciencedirect.com
SCIENCE DIRECT®
Biochemical and Biophysical Research Communications 337 (2005) 22–29
BBRC
www.elsevier.com/locate/ybbrc

Interaction of measles virus vectors with Auger electron emitting radioisotopes

David Dingli [a,b,*], Kah-Whye Peng [a], Mary E. Harvey [a], Sompong Vongpunsawad [a], Elizabeth R. Bergert [c], Robert A. Kyle [b], Roberto Cattaneo [a], John C. Morris [c], Stephen J. Russell [a,b]

[a] *Molecular Medicine Program, Mayo Clinic College of Medicine, Rochester, MN 55905, USA*
[b] *Division of Hematology, Mayo Clinic College of Medicine, Rochester, MN 55905, USA*
[c] *Division of Endocrinology, Diabetes, Metabolism, Nutrition and Internal Medicine, Mayo Clinic College of Medicine, Rochester, MN 55905, USA*

Received 19 August 2005
Available online 13 September 2005

Abstract

A recombinant measles virus (MV) expressing the sodium iodide symporter (NIS) is being considered for therapy of advanced multiple myeloma. Auger electrons selectively damage cells in which the isotope decays. We hypothesized that the Auger electron emitting isotope ^{125}I can be used to control viral proliferation. MV was engineered to express both carcinoembryonic antigen and NIS (MV-NICE). Cells were infected with MV-NICE and exposed to ^{125}I with appropriate controls. MV-NICE replication in vitro is inhibited by the selective uptake of ^{125}I by cells expressing NIS. Auger electron damage is partly mediated by free radicals and abrogated by glutathione. In myeloma xenografts, control of MV-NICE with ^{125}I was not possible under the conditions of the experiment. MV-NICE does not replicate faster in the presence of radiation. Auger electron emitting isotopes effectively stop propagation of MV vectors expressing NIS in vitro. Additional work is necessary to translate these observations in vivo.

Keywords: Virotherapy; Multiple myeloma; Sodium iodide symporter; Iodide; Auger electron

Recombinant, replication competent viruses based on the vaccine strain of measles virus (MV-Edm) are emerging as powerful oncolytic viruses with the potential to treat a wide variety of tumors in animal models [1–4]. MV-Edm binds to cells when the viral hemagglutinin (H) protein engages the CD46 receptor present on target cells that triggers conformational changes in the fusion (F) protein and membrane mixing. The vast majority of tumor cells overexpress CD46 and thus, MV-Edm based viruses have a natural tropism for tumor cells. The cytopathic effect of the virus in cell-to-cell fusion depends in part on the density of CD46 expression [5]. Tumor cell lines exposed to MV-Edm in vitro are uniformly destroyed by the tumor but in vivo, responses to MV-Edm are more variable and some tumors persist despite repeated doses of the virus. In order to better understand the outcome of these experiments, recombinant viruses that induce the expression of inert, soluble marker peptides such as carcinoembryonic antigen (CEA) or the beta chain of human chorionic gonadotrophin (β-hCG) were generated [6]. Administration of these viruses in tumor bearing mice led to the expression of the respective protein that could be measured using available assays. In vivo studies with these viruses showed persistent virus replication in the presence of ongoing tumor growth. In order to enhance the oncolytic potential of the virus, MV-Edm was engineered to induce the expression of the thyroidal sodium iodide symporter (NIS) in infected cells (MV-NIS) [7]. MV-NIS replication and spread as well as gene expression can be monitored non-invasively by the administration of radioactive iodide isotopes and the appropriate imaging modality (gamma camera or positron

* Corresponding author. Fax: +1 507 284 8388.
E-mail address: dingli.david@mayo.edu (D. Dingli).

0006-291X/$ - see front matter © 2005 Elsevier Inc. All rights reserved.
doi:10.1016/j.bbrc.2005.08.261

emission tomography) [7]. In addition, MV-NIS in combination with ^{131}I can eliminate tumors that are otherwise resistant to the virus itself [7].

MV-NIS has been approved by the Recombinant DNA Advisory Committee (RAC) for a Phase I study in patients with advanced or refractory multiple myeloma. The virus was rescued from a plasmid with an MV genome derived largely from a vaccine related laboratory strain. MV vaccines have been administered to millions of people with an excellent safety record. Children are vaccinated after the age of 15 months in countries with a low incidence of measles and earlier in nations with a high incidence of the disease in attempts to prevent spread of the illness [8].

Patients with myeloma are significantly immunocompromised with defects both in the humoral as well as the cellular arms of the immune system [9,10]. Virus inactivation in the circulation might be low in patients with myeloma due to low levels of anti-MV neutralizing antibody. While this may be advantageous during systemic administration of the vector, the poor immune response raises concerns regarding unchecked virus replication in patients with the disease. In patients with hematological malignancies or HIV infection, wild type measles virus infection is particularly severe, associated with a high incidence of complications and a mortality rate approaching 70% [11].

The number of pharmacologic agents with activity against measles virus is limited. While in vitro studies suggest that ribavirin has substantial activity against the virus, clinical data supporting the use of this drug are based essentially on case reports [12]. Intravenous immune globulin is available and has significant activity and anecdotal reports suggest that the combination of immune globulin and ribavirin may be effective in immunocompromised patients [13].

Cells that have been irradiated are more susceptible to the cytopathic effect of viruses. Both DNA (e.g., adenovirus) as well as RNA viruses (e.g., measles, NDV, and poliovirus) replicate to higher titers in cells that have been exposed to electromagnetic radiation [14]. Radiation can also dampen the immune response against viruses and thus enhance spread of the virus [15]. In principle, damage from viral proliferation can be limited by strategies to retarget recombinant measles viruses for selective infection of tumor cells [16–20].

Exposure of infected cells to radiation can however damage progeny genomes and impede spread of the virus in tumors. The relatively long path length of electrons emitted by ^{131}I will most likely be deposited outside the cell from where they originated although (contributing too the bystander effect) [21], although electron cross-fire has to be considered. If radiation damage can be confined to infected cells, it may be possible to use this to control viral proliferation. Auger electron emitters, concentrated exclusively in MV-NIS infected cells, may be the key to achieving this goal since their electrons have very short path length (<1 μm).

Radioactive isotopes can lose an inner shell electron either by a process of electron capture or by a process of internal conversion whereby a gamma photon emitted from the nucleus is absorbed by an inner shell electron that is then ejected [22]. Either process creates a vacancy in the inner shell that is filled by an electron from an outer shell. This is associated with the release of energy that can be transmitted to another electron in the same or higher orbital that can also be emitted. Thus, a cascade of electron emissions are generated that are in general referred to as Auger electrons [23]. Their energies vary from several electron volts to tens of kilo-electron volts. As a consequence, their path length in biological systems is usually in the nanometer range (subcellular). However, the large number of electrons emitted by these processes means that local high energy densities can be achieved and it has been calculated that 1 MGy is absorbed within 1–2 nm from the decay site per disintegration [24]. Thus, Auger electrons have high linear energy transfer with the potential to induce considerable damage within very short distances after they are generated. Many radionuclides emit Auger electrons including a number that are routinely used in clinical practice such as ^{99m}Tc, ^{111}In, and ^{123}I. ^{125}I is a prolific Auger electron emitter with an average of 25 electron emissions per decay [23]. The mean energy of the electrons emitted by the decay of ^{125}I is less than 1 keV [24]. ^{123}I also emits approximately 15 Auger electron when it decays [23].

The short path length of Auger electrons imposes spatial constraints on their biological activity. Various studies have demonstrated that unless the isotope decays in the cytoplasm and preferably in the nucleus of the cell, Auger emitting isotopes may not be an effective form of targeted radiation for tumor therapy [24,25]. Thus, we hypothesized that it might be possible to utilize Auger electron-emitting iodide isotopes to selectively destroy virus-infected cells and stop virus propagation. We report on our studies of this approach both in vitro and in vivo with ^{125}I.

Methods

Generation of recombinant MV expressing CEA and NIS (MV-NICE). Plasmids p(+) MV-CEA and p(+) MV-NIS have been described elsewhere [6,7]. Both plasmids were both digested with *Sac*II and *Not*I. The 7025 bp product from digestion of p(+) MV-CEA and the 16,125 bp product from the digestion of p(+) MV-NIS were gel purified and ligated to generate plasmid p(+) MV-NICE. The recombinant virus was rescued by contransfection of 293-3-46 cells with plasmids p(+) MV-NICE (5 μg) and pEMCLa (50 ng) using calcium phosphate precipitation [26]. After 3 days, the producer cells were overlaid on Vero cells and rescue inferred by the observation of syncytium formation. Individual syncytia were isolated, lysed by vortexing, and used to infect new Vero cells. Cell associated virus was released by freeze–thawing the cells twice in liquid nitrogen and cell lysates were cleared by centrifugation. For titration of virus stocks, serial logarithmic dilutions of the virus were used to infect Vero cells in 96-well plates and the 50% tissue culture infective dose ($TCID_{50}$/ml) was determined after 96 h as described by Spearman and Karber. One-step growth curves were determined by infecting Vero cells in six-well plates at an MOI of 3. Infected cells were maintained at 32 °C and samples were harvested every 12 h in Opti-MEM for titration of cell associated virus.

Cell lines. ARH-77 cells and Vero cells were obtained from the American Type Culture Collection (ATCC, Manassas, VA) while MM1 cells were a generous gift of Dr Rafael Fonseca (Mayo Clinic Rochester).

ARH-77 and MM1 cells were maintained in RPMI 1640 with 10% fetal bovine serum (FBS) while Vero cells were maintained in DMEM with 10% FBS. All cell lines were kept in humidified incubators at 37 °C with 5% carbon dioxide. Cell culture media were from Cellgro (Mediatech, Herndon, VA).

In vitro studies with MV-NICE. ARH-77 cells were plated at a density of 5×10^5/ml of medium and infected with MV-NICE or MV-Edm at an MOI of 0.02. Starting 48 h after infection, conditioned media as well as the cells were harvested and tested for CEA production (Central Clinical Laboratory, Mayo Clinic, Rochester) and for NIS expression by in vitro iodide uptake as previously described [7,18].

In order to study the potential of Auger electrons emitters in controlling MV-NICE replication, ARH-77 cells were infected with MV-NICE or MV-CEA (control) at an MOI of 0.02 for 2 h (in Opti-MEM) and then maintained under the following four conditions: RPMI with 10% FBS, RPMI with 10% FBS and $KClO_4$ (100 μM), RPMI with 10% FBS supplemented with $Na^{125}I$ with an activity of 3.7 MBq/ml, and RPMI with 10% FBS supplemented with both $Na^{125}I$ and $KClO_4$ (100 μM). Starting 12 h after infection, conditioned media and cells were harvested. The cells were decontaminated from the isotope by incubating them for 20 min three times with RPMI/10% FBS and $KClO_4$ (100 μM). After the final wash, the cells were resuspended in Opti-MEM and frozen at −80 °C. At the end of the experiment, all the cells were lysed by freeze–thawing twice in liquid nitrogen. The titer of cell-associated virus from cleared cell lysates were obtained by serial dilution and infection of Vero cells. Similar experiments were performed with glutathione (GSH) (Sigma, St. Louis, MI) substituting for $KClO_4$. GSH, a free radical scavenger, was used at a concentration of 7 mM [27].

Removal of ^{125}I from cell-conditioned media. Since ^{125}I has a half-life of 60 days, cell-conditioned media were desalted by size exclusion chromatography through Sepharose-G25 PD-10 columns (Amersham Pharmacia, Piscataway, NJ) after equilibrating the columns with serum free RPMI 1640. In order to harvest the correct fractions with minimal radioiodide, a trial run with 1 ml of conditioned medium was spiked with $Na^{125}I$ (1×10^5 cpm total) and loaded onto the column. Serial 1 ml fractions were collected and analyzed both for protein content by ultraviolet absorbance (280 nm) and gamma photon emission. The fractions with highest content of protein and minimal iodide contamination were identified and the same fractions from all cell-conditioned media were collected for CEA estimation.

Neutralizing antibody assay for measles virus. After approval from the Institutional Review Board at Mayo Clinic and in accordance with federal regulations, we obtained stored sera from patients with monoclonal gammopathy of undetermined significance (MGUS), patients with advanced myeloma, and patients who had undergone autologous stem cell transplantation (ASCT) for myeloma as well as normal age-matched controls. Sera were evaluated for the presence of anti-measles virus antibodies at the Serology Laboratory, Mayo Clinic Rochester.

In vivo studies with MV-NICE. Sixteen 6-week-old female CB17scid mice (Harlan Sprague–Dawley, Madison, WI) were given total body irradiation (250 cGy). Twenty-four hours later, they were injected in their right flank with washed MM1 cells (1×10^7). The mice were fed levothyroxine in their drinking water (5 mg/L) to suppress thyroidal NIS expression. Tumor growth was measured in two dimensions with calipers and when the tumors reached a mean diameter of 0.6 cm, 8 mice (Group A) were injected intravenously with MV-CEA (2×10^6 $TCID_{50}$/ml) and another 8 mice (Group B) were injected with MV-NICE (2×10^6 $TCID_{50}$/ml). Four days later 4 mice from each group were injected intraperitoneally with $Na^{125}I$ (37 MBq). All 16 mice were bled 7 and 11 days after isotope injection for CEA estimation. The mice were euthanized if the tumors ulcerated, if they grew to more than 10% of the weight of the animal or if the tumors interfered with feeding or drinking. The study was approved by the Institutional Animal Care and Use Committee (IACUC) at Mayo Clinic.

Statistical analysis. All statistical analyses were performed using StatView software. Student's t test was used to evaluate the difference in means with a p value <0.05 being considered significant. Correlations were performed with Spearman's test.

Results

Neutralizing anti-measles virus antibodies in patients with myeloma

Since patients with myeloma are often immunocompromised, we wanted to quantify the level of neutralizing anti-measles virus antibody. This is important when a replicating measles virus is being considered for systemic therapy in these patients. High levels of neutralizing antibodies may rapidly inactivate the virus upon administration while low levels of immunity may allow unhindered virus proliferation. Thus, we obtained sera from patients with MGUS, advanced myeloma, and patients with myeloma who have undergone autologous stem cell transplantation (ASCT) at least a year before and compared them to age matched controls. Patients with advanced myeloma or after ASCT have significantly lower levels of anti-measles virus antibodies compared to age matched controls or patients with MGUS (Fig. 1; $p = 0.01$ for myeloma and $p = 0.0068$ for patients after ASCT). Due to these observations and given that MV-NIS will be combined with radioisotopes for imaging, we wanted to understand the behavior of the virus in the presence of radiation and explore the possible use of low energy (Auger) electron emitters to control virus propagation.

Rescue and characterization of MV-NICE

Since we were interested in monitoring both in vitro and in vivo virus propagation in the presence of ^{125}I, we opted to engineer a replicating MV coding both for NIS as well as the soluble form of human CEA (MV-NICE). In this way, viral gene expression could be monitored using CEA production. A plasmid coding for the full-length genome was generated and rescued as described under Methods (Fig. 2A). Parallel one-step growth curves for MV-Edm and MV-NICE show that the virus propagates slower than

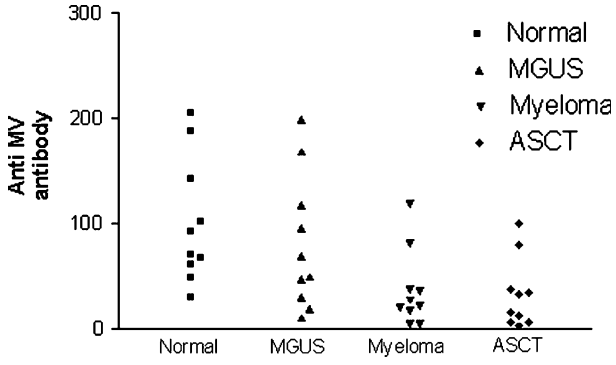

Fig. 1. Anti-measles virus neutralizing antibodies in patients with plasma cell disorders and age matched controls. Forty adults were studied including 10 healthy adults, and 10 patients each with MGUS, advanced myeloma and patients 1 year after ASCT for myeloma. Antibody titers in patients with advanced myeloma and after ASCT are significantly lower than those in control subjects ($p = 0.01$ and 0.0068, respectively).

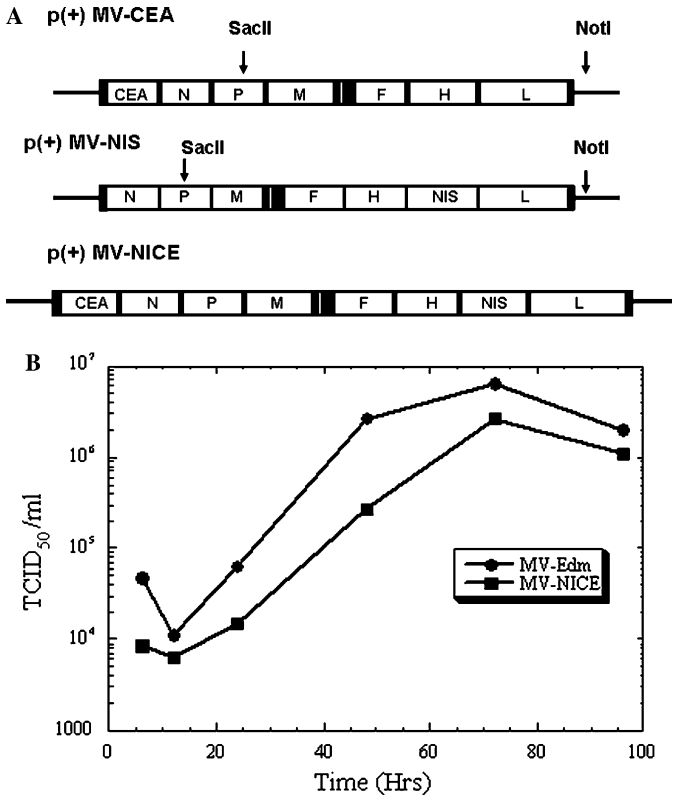

Fig. 2. (A) Schematic representation of the genomes of the viruses used in this study. (B) One-step growth curves for cell associated virus show that MV-NICE propagates slower than MV-Edm and to somewhat lower titers.

MV-Edm and reaches slightly lower titers (Fig. 2B). ARH-77 cells infected with MV-NICE express NIS, concentrate radioiodine in vitro, and secrete CEA (Fig. 3). The presence of perchlorate has no effect on virus proliferation and CEA production. Both NIS expression and CEA production increase with time as the viral infection spreads in the culture. There is a close correlation between iodide uptake and CEA production (Spearman's ρ: 0.99, $p < 0.05$) indicating that expression of the two genes is concordant.

In vitro MV-NICE control

We wanted to study the behavior of MV in the presence of radiation and explore the potential of Auger electrons emitted by ^{125}I to control virus propagation in a culture system. ARH-77 cells were infected either with MV-NICE or MV-CEA at an MOI of 0.02 for 2 h. The cells were infected in a single tube as a "master mix" in Opti-MEM to minimize variation in infection rates. After the 2-h incubation with virus, the cells were centrifuged and aliquoted at 1×10^5 cells in 1 ml medium with or without $KClO_4$ (100 μm) and with or without $Na^{125}I$ (3.7 MBq/ml, final concentration). Every 12 h conditioned media and cells were harvested, decontaminated as described, and tested for CEA production as well as virus production by titration on Vero cells. We used CEA levels as a surrogate for viral

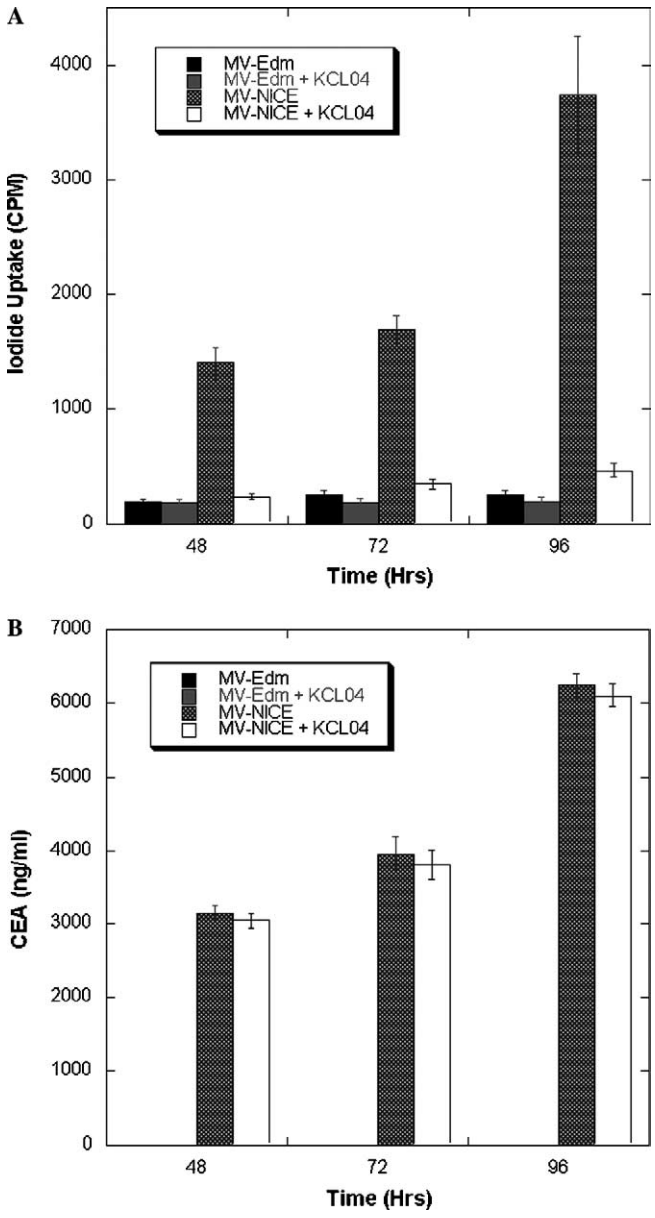

Fig. 3. Characterization of MV-NICE. ARH-77 cells infected with MV-NICE express NIS and concentrate radioiodide (A) and secrete CEA into the media. Cells infected with MV-Edm do not express NIS and do not induce secretion of CEA. (B) Both NIS expression and CEA production increase with time due to virus propagation. NIS and CEA expression is tightly correlated (Spearman's ρ: 0.99, $p < 0.05$).

gene expression. Viable virus generation was studied by titration of serial dilutions of cell lysates on Vero cells.

The presence of ^{125}I or $KClO_4$ in the media had no effect on CEA production and virus propagation in the MV-CEA infected culture (Figs. 4A and B). MV-NICE infects myeloma cells and they start secreting CEA; levels of the protein increase with time (Fig. 4C). CEA production is significantly lower in conditioned media from MV-NICE infected cells in the presence of ^{125}I but the isotope has no effect if it is prevented from entering virus-infected cells by perchlorate (Fig. 4C). Titration of cell lysates confirmed that no viable virus was produced in the presence of

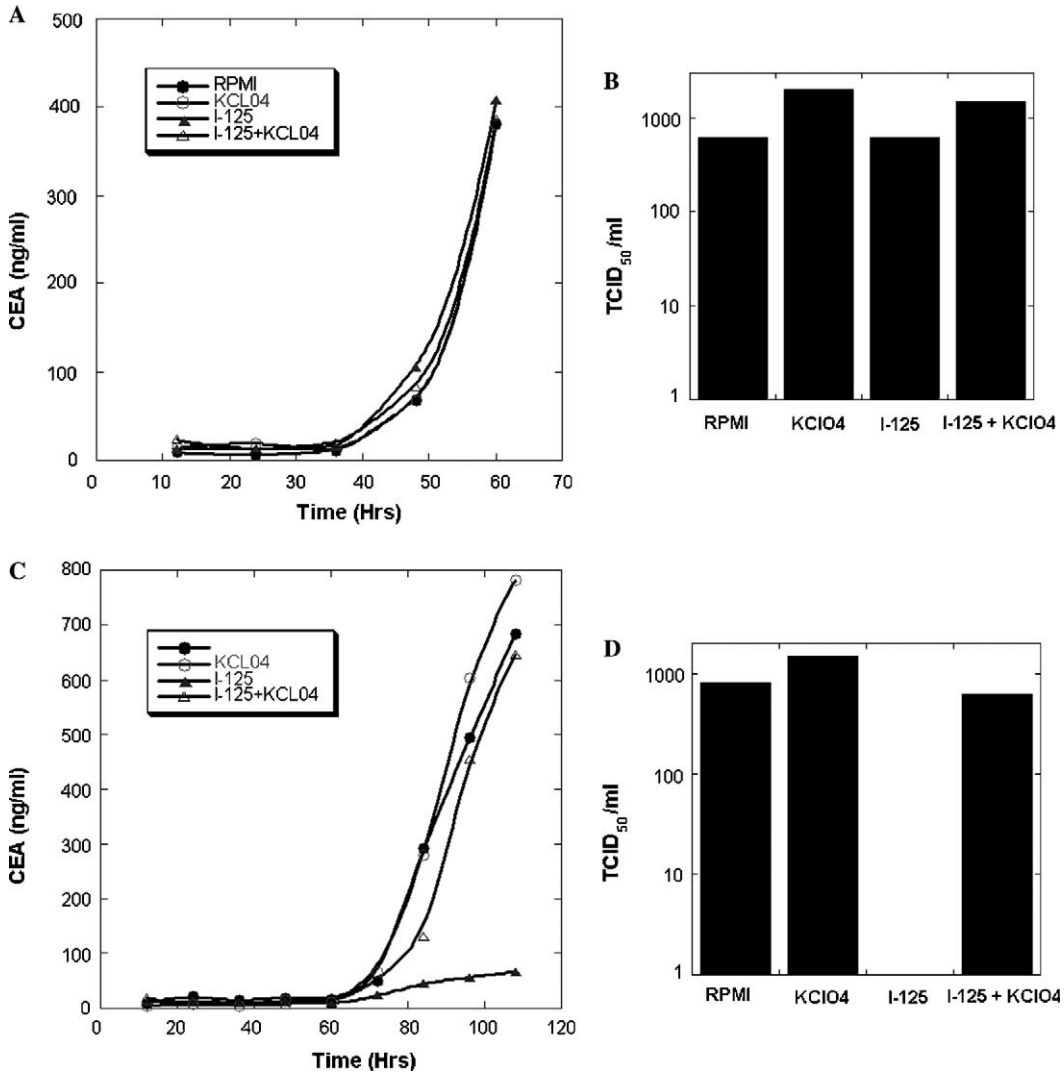

Fig. 4. In vitro control of MV-NICE with ^{125}I. MV-CEA gene expression (A) and virus generation (B) are virtually identical in the presence or absence of ^{125}I. Cells infected with MV-NICE produce small amounts of CEA (C) in the presence of the isotope and this is mirrored by undetectable virus generation (D). However, if the isotope is prevented from entering the cells by perchlorate, both CEA and viable virus are produced (C,D). Therefore, the isotope has to decay within the cell for it to have an effect on virus propagation. The viral titers shown are at 60 h for MV-CEA and 96 h for MV-NICE.

intracellular ^{125}I (Fig. 4D). Thus, it appears that if cells express NIS and concentrate ^{125}I intracellularly, virus replication can be stopped. However, the presence of the isotope in the media has no effect on CEA production and virus propagation in the MV-CEA infected culture, confirming that both NIS expression and intracellular isotope decay are necessary for inhibition of virus proliferation.

Auger electron damage is mediated by free radicals

Decay of ^{125}I in the cell leads to the generation of free radicals and reactive oxygen species. These induce cell death by activation of the mitochondrial apoptotic pathway [28]. Therefore, if free radical scavengers are added to the cell culture media, the virus and virus infected cells might be protected from the effect of ionizing radiation. To evaluate this possibility, we infected ARH-77 cells with MV-NICE (MOI: 0.02) and incubated the cells with ^{125}I in the presence or absence of glutathione, a free radical scavenger that is taken up by cells [29]. In the presence of glutathione, infected cells produce CEA and detectable amounts of virus although the levels are not the same as in cells not exposed to the isotope (Figs. 5A and B). We conclude that free radicals are, in part, responsible for the damage to virus infected cells and viral genomes induced by ^{125}I.

Control of MV-NICE in a myeloma xenograft model

We then attempted to inhibit viral replication with ^{125}I in vivo in a myeloma xenograft model. We detected CEA production after the systemic administration of MV-NICE (2×10^6 $TCID_{50}$/ml) in SCID mice bearing MM1 myeloma tumor xenografts. CEA levels increased with time as the

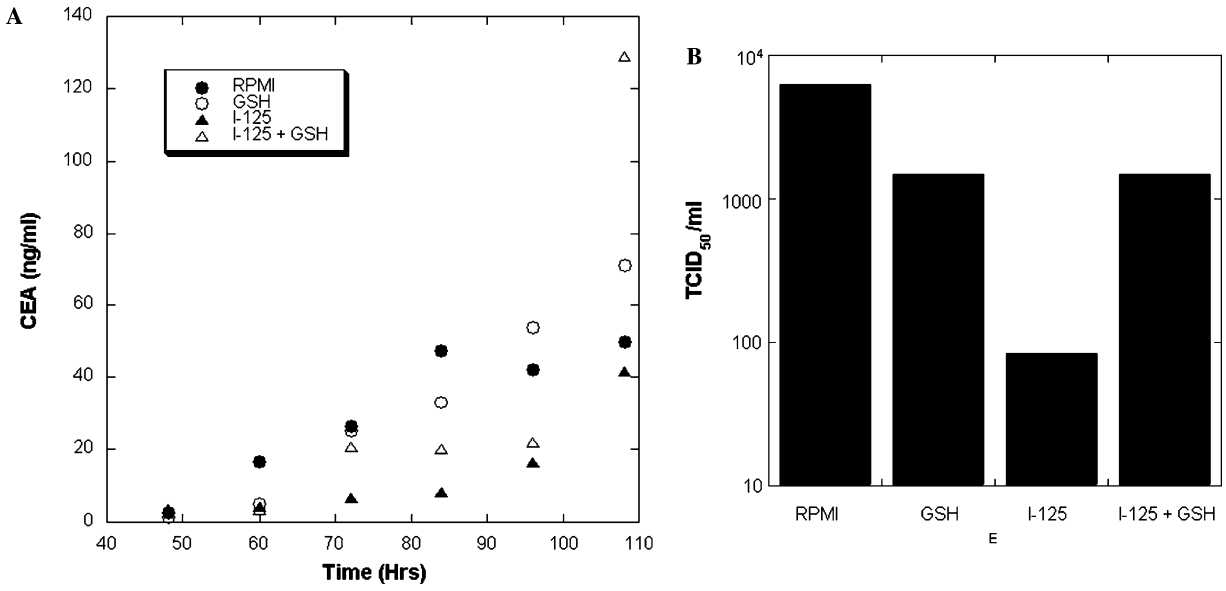

Fig. 5. Auger electron damage is via free radical generation. (A) CEA production is not affected by GSH. The presence of the free radical scavenger protects cells from damage with ^{125}I and CEA production being higher. (B) Glutathione protects MV-NICE from the effect of ^{125}I and some viable virus is detectable in the presence of the scavenger.

virus replicated and spread in the tumor (data not shown). Once the CEA profile was available, we attempted in vivo control of MV-NICE with ^{125}I. Sixteen female SCID mice were implanted with MM1 cells after TBI. Eight mice were injected with MV-CEA (2×10^6 $TCID_{50}$/ml) and the other eight with MV-NICE (same dose) via tail vein injection. Four days later, four mice from each group were treated with ^{125}I (37 MBq, intraperitoneally). The mice were bled for CEA estimation 7 and 11 days after isotope injection (Fig. 6A). Blood levels for the marker peptide, on day 7 and 11, are presented in Figs. 6B–E. In general, CEA levels increased with time in all mice. As expected, ^{125}I had no effect on MV-CEA but perhaps surprisingly, it had no effect on MV-NICE propagation either. The potential reasons behind this result are discussed in the next section.

Discussion

The vaccine strain of MV has an excellent safety record since it has been given to millions of people without serious problems [8]. However, systemic administration of a replication competent virus in an immunocompromised host requires some mechanism to halt viral proliferation because of the risk of uncontrolled infection. Apart from anti-MV immune globulin, there is no proven pharmacotherapy for MV. Viruses have been reported to proliferate at higher rates in the presence of radiation; a phenomenon that may increase the potential danger of MV-NIS when combined with radioactive iodide for therapy [14]. It is also possible that radiation from ^{131}I decay may dampen an immune response against the virus and further increase the risk of uncontrolled viral proliferation.

We have studied the behavior of MV in the presence of radiation and under the conditions of our experiments, MV derived vectors engineered to express NIS do not proliferate any faster in the presence of radiation in ARH-77 cells. Our in vitro data suggest that it might be possible to use low energy Auger electron emitters to halt virus generation. No viable MV-NICE was grown from cell lysates in the presence of the isotope whereas MV-CEA was generated to titers comparable to the controls with similar CEA levels. Therefore, NIS expression is necessary for the isotope to stop virus propagation; the mere presence of isotope in the medium is not enough for therapy. This is in keeping with the known radiobiology of Auger electron emitters; unless the isotope decays in the cytoplasm or preferably in the nucleus of a cell, these electrons have minimal effects on cell viability [29]. The short path length and the necessity for intra-cytoplasmic decay make Auger electron emitters such as ^{125}I, an attractive strategy for vector control since radiation damage will be virtually restricted to infected cells.

Both ^{123}I and $^{99m}TcO_4$ emit Auger electrons (15 and 4 per decay, respectively) and therefore potentially might interfere with virus proliferation in vivo [23]. This may be a concern during in vivo experiments and more so in clinical studies when these isotopes might be used to monitor non-invasively and repeatedly viral gene expression and vector propagation. Theoretical calculations suggest that for imaging purposes, $^{99m}TcO_4$ is the isotope of choice; it emits a smaller number of electrons and the mean energy of the emitted electrons is even lower than those emitted from ^{123}I (0.899 and 27.5 keV, respectively) [23]. Indeed, assuming that the biological half-life of the three isotopes in an infected cell is the same, the relative risk of cellular damage as a function of isotope decay is $376.8 > 34.15 > 1.33$ for ^{123}I, $^{99m}TcO_4$, and ^{125}I, respectively.

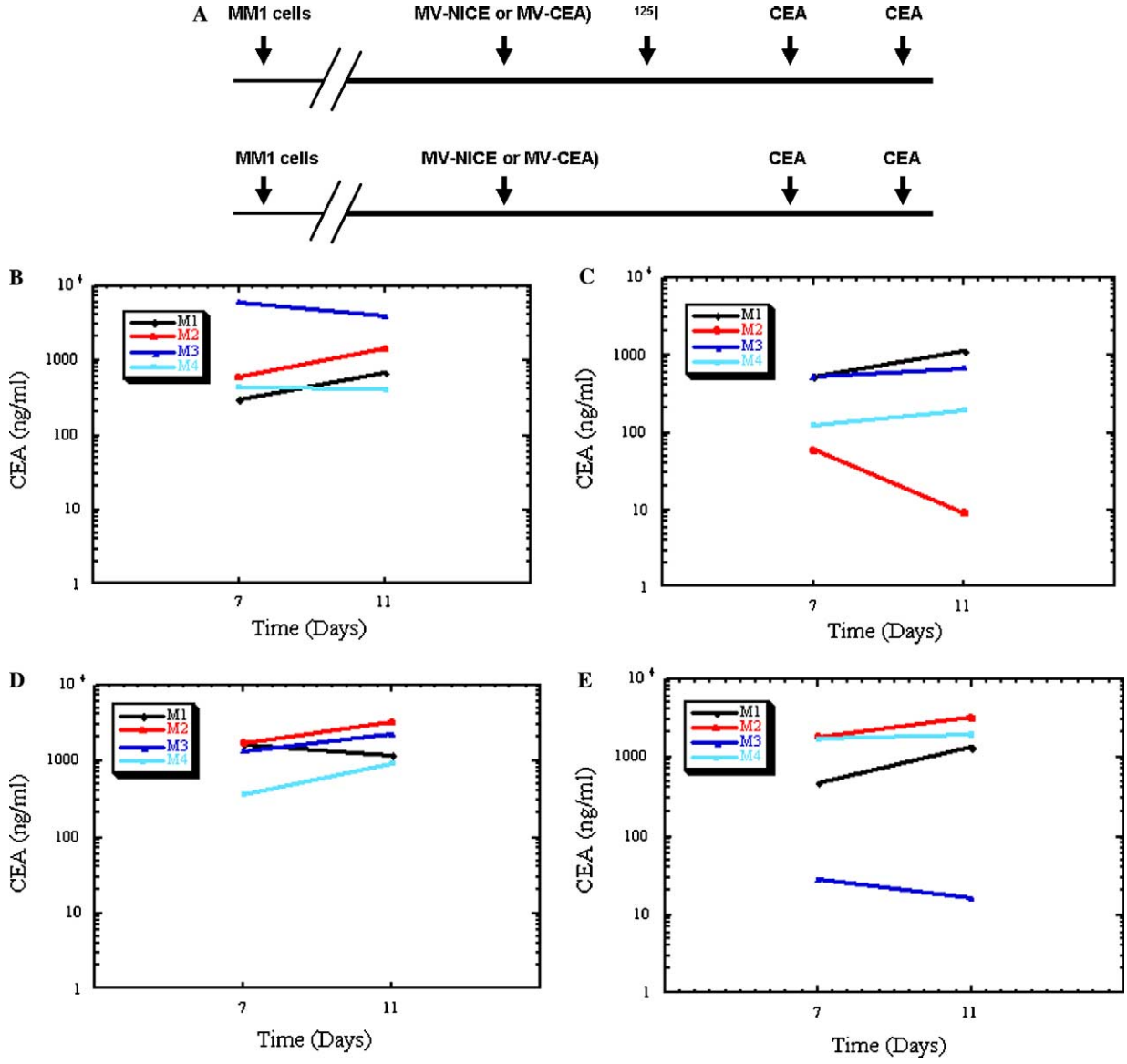

Fig. 6. CEA levels on days 7 and 11 in MM1 xenograft bearing SCID mice. (A) Experimental design with MM1 tumors implanted in SCID mice and injected intravenously either with MV-CEA or MV-NICE when the tumors reached a mean diameter of 0.6 cm. The mice in (B,C) were injected with MV-CEA while those in (D,E) were injected with MV-NICE (2×10^6 $TCID_{50}$/ml) intravenously. Four days later, the mice in (C,E) were treated with $Na^{125}I$ (37 MBq, intraperitoneally,) and bled 7 and 11 days later.

To our knowledge, this is the first reported attempt to use the physical characteristics of Auger electrons to control an engineered replication competent vector that will be undergoing Phase I studies in the near future. Our initial attempts to stop virus propagation in vivo failed. There are a number of possible explanations for the outcome of this experiment that can be divided into kinetic or energetic. It might be possible that there is a small window of opportunity for therapy to work; if viral proliferation is fast relative to cell death it might be difficult to eliminate viral propagation (kinetic problem). Thus, the potential interaction between the rate of virus proliferation and timing of therapy needs to be further explored.

The other major consideration relates to energy deposition by the intracellular decay of the isotope in virus-infected cells. Cells need to accumulate a critical amount of damage before they undergo apoptosis. Cellular damage is a function of the energy deposited in the cell that in turn is a function of the number of disintegrations that occur within that cell [24]. Thus, it is possible that not enough isotope was injected in the mice or the levels of NIS expression were not high enough for adequate intracellular iodide accumulation. The isotope must be retained in the tumor for sufficient time to ensure that enough disintegrations occur in the cell. Isotope uptake and retention is a dynamic process that is in part determined by the level of NIS expression [30]. Clearly, the virus infected the cells and considerable amounts of CEA were generated and therefore NIS was expressed. The effective half-life of the isotope in the tumor is a critical determinant of

the outcome of therapy. Preliminary calculations suggest that indeed, this might have been a crucial factor. A short retention time compared to the physical half-life of the isotope means that most of the isotope leaks from inside cells without decay and therefore has no impact on cell or virus survival. Strategies to enhance isotope retention or the use of Auger electron emitting isotopes with a shorter physical half-life may solve this problem. In addition, strategies to retarget recombinant measles viruses for infection of tumor cells selectively will add significantly to the safety of these vectors in vivo.

Acknowledgments

This work was supported by Grant CA100634 from the NCI (S.J.R.) and a fellowship from the Multiple Myeloma Research Foundation (D.D.).

References

[1] K.W. Peng, G.J. Ahmann, L. Pham, P.R. Greipp, R. Cattaneo, S.J. Russell, Systemic therapy of myeloma xenografts by an attenuated measles virus, Blood 98 (2001) 2002.
[2] D. Grote, S.J. Russell, T.I. Cornu, R. Cattaneo, R. Vile, G.A. Poland, A.K. Fielding, Live attenuated measles virus induces regression of human lymphoma xenografts in immunodeficient mice, Blood 97 (2001) 3746.
[3] K.W. Peng, C.J. TenEyck, E. Galanis, K.R. Kalli, L.C. Hartmann, S.J. Russell, Intraperitoneal therapy of ovarian cancer using an engineered measles virus, Cancer Res. 62 (2002) 4656.
[4] L.K. Phuong, C. Allen, K.W. Peng, C. Giannini, S. Greiner, C.J. TenEyck, P.K. Mishra, S.I. Macura, S.J. Russell, E.C. Galanis, Use of a vaccine strain of measles virus genetically engineered to produce carcinoembryonic antigen as a novel therapeutic agent against glioblastoma multiforme, Cancer Res. 63 (2003) 2462.
[5] B.D. Anderson, T. Nakamura, S.J. Russell, K.W. Peng, High CD46 receptor density determines preferential killing of tumor cells by oncolytic measles virus, Cancer Res. 64 (2004) 4919.
[6] K.W. Peng, S. Facteau, T. Wegman, D. O'Kane, S.J. Russell, Non-invasive in vivo monitoring of trackable viruses expressing soluble marker peptides, Nat. Med. 8 (2002) 527.
[7] D. Dingli, K.W. Peng, M.E. Harvey, P.R. Greipp, M.K. O'Connor, R. Cattaneo, J.C. Morris, S.J. Russell, Image-guided radiovirotherapy for multiple myeloma using a recombinant measles virus expressing the thyroidal sodium iodide symporter, Blood 103 (2004) 1641.
[8] F.T. Cutts, L.E. Markowitz, Successes and failures in measles control, J. Infect. Dis. 170 (Suppl. 1) (1994) S32.
[9] J.A. Katzmann, Myeloma-induced immunosuppression: a multistep mechanism, J. Immunol. 121 (1978) 1405.
[10] D.R. Jacobson, S. Zolla-Pazner, Immunosuppression and infection in multiple myeloma, Sem. Oncol. 13 (1986) 282.
[11] L.J. Kaplan, R.S. Daum, M. Smaron, C.A. McCarthy, Severe measles in immunocompromised patients, J. Am. Med. Assoc. 267 (1992) 1237.
[12] M. Hosoya, S. Shigeta, S. Mori, A. Tomoda, S. Shiraishi, T. Miike, H. Suzuki, High-dose intravenous ribavirin therapy for subacute sclerosing panencephalitis, Antimicrob. Agents Chemother. 45 (2001) 943.
[13] S.W. Stogner, J.W. King, C. Black-Payne, J. Bocchini, Ribavirin and intravenous immune globulin therapy for measles pneumonia in HIV infection, South. Med. J. 86 (1993) 1415.
[14] S. Levine, Effects of irradiation on the responses of animal cells to virus, Prog. Med. Virol. 16 (1973) 157.
[15] H. Blomgren, R. Berg, J. Wasserman, U. Glas, Effect of radiotherapy on blood lymphocyte population in mammary carcinoma, Int. J. Radiat. Oncol. Biol. Phys. 1 (1976) 177.
[16] T. Nakamura, K.W. Peng, S. Vongpunsawad, M. Harvey, H. Mizuguchi, T. Hayakawa, R. Cattaneo, S.J. Russell, Antibody-targeted cell fusion, Nat. Biotechnol. 22 (2004) 331.
[17] E.M. Hadac, K.W. Peng, T. Nakamura, S.J. Russell, Reengineering paramyxovirus tropism, Virology 329 (2004) 217.
[18] U. Schneider, F. Bullough, S. Vongpunsawad, S.J. Russell, R. Cattaneo, Recombinant measles viruses efficiently entering cells through targeted receptors, J. Virol. 74 (2000) 9928.
[19] A.L. Hammond, R.K. Plemper, J. Zhang, U. Schneider, S.J. Russell, R. Cattaneo, Single-chain antibody displayed on a recombinant measles virus confers entry through the tumor-associated carcinoembryonic antigen, J. Virol. 75 (2001) 2087.
[20] S. Vongpunsawad, N. Oezgun, W. Braun, R. Cattaneo, Selectively receptor-blind measles viruses: identification of residues necessary for SLAM- or CD46-induced fusion and their localization on a new hemagglutinin structural model, J. Virol. 78 (2004) 302.
[21] D. Dingli, S.J. Russell, J.C. Morris III, In vivo imaging and tumor therapy with the sodium iodide symporter, J. Cell. Biochem. 90 (2003) 1079.
[22] J.M. Blatt, V.F. Weiskopf, Theoretical Nuclear Physics, Dover Publications, New York, 1991.
[23] J.A. O'Donoghue, T.E. Wheldon, Targeted radiotherapy using Auger electron emitters, Phys. Med. Biol. 41 (1996) 1973.
[24] K.S. Sastry, Biological effects of the Auger emitter iodine-125: a review. Report No. 1 of AAPM Nuclear Medicine Task Group No. 6 (see comment). Med. Phys. 19 (1992) 1361.
[25] A.I. Kassis, F. Fayad, B.M. Kinsey, K.S. Sastry, R.A. Taube, S.J. Adelstein, Radiotoxicity of 125I in mammalian cells, Radiat. Res. 111 (1987) 305.
[26] F. Radecke, P. Spielhofer, H. Schneider, K. Kaelin, M. Huber, C. Dotsch, G. Christiansen, M.A. Billeter, Rescue of measles viruses from cloned DNA, EMBO J. 14 (1995) 5773.
[27] M.T. Vlachaki, R.E. Meyn, ASTRO research fellowship: the role of BCL-2 and glutathione in an antioxidant pathway to prevent radiation-induced apoptosis, Int. J. Radiat. Oncol. Biol. Phys. 42 (1998) 185.
[28] C. Ferlini, R. D'Amelio, G. Scambia, Apoptosis induced by ionizing radiation. The biological basis of radiosensitivity, Subcell. Biochem. 36 (2002) 171.
[29] D.V. Rao, V.R. Narra, R.W. Howell, K.S. Sastry, Biological consequence of nuclear versus cytoplasmic decays of 125I: cysteamine as a radioprotector against Auger cascades in vivo, Radiat. Res. 124 (1990) 188.
[30] D. Dingli, E.R. Bergert, Z. Bajzer, M.K. O'Connor, S.J. Russell, J.C. Morris, Dynamic iodide trapping by tumor cells expressing the thyroidal sodium iodide symporter, Biochem. Biophys. Res. Commun. 325 (2004) 157.